Research Article

Advances in Mechanical Engineering

Advances in Mechanical Engineering
2018, Vol. 10(8) 1–11

DOI: 10.1177/1687814018796008
journals.sagepub.com/home/ade
SAGE

Modification of boundary condition for the optimization of natural frequencies of plate structures with fluid loading

Dayi Ou[1] and Cheuk Ming Mak[2]

Abstract

A finite element method, boundary element method, and genetic algorithm combined method is developed for the optimization of natural frequencies of fluid-loaded plates. In this method, the coupled finite element method–boundary element method is used for the free flexural vibration analysis of plates with arbitrary fluid loading effects and arbitrary elastic boundary conditions, and the genetic algorithm method is combined with the finite element method–boundary element method for searching the optimal values of plate's boundary parameters. By using this method, multiple natural frequencies of a given fluid-loaded plate can be optimized simultaneously to different target values. The coupled finite element method–boundary element method is first validated by comparing with earlier published results. The proposed optimization method is then applied to the optimal boundary condition design of four different cases. The results show natural frequencies of a fluid-loaded plate are sensitive to its boundary conditions. The possibility of optimizing the natural frequencies of a fluid-loaded plate by modifying boundary conditions is demonstrated, as well as the effectiveness of the proposed method as a structural optimization tool. According to the authors' knowledge, this study is the first attempt of optimizing fluid-loaded plate natural frequencies by considering arbitrary boundary conditions as optimization variables.

Keywords

Natural frequencies, fluid loading effects, plate structure, boundary condition, optimization, fluid mechanics, finite element analysis, boundary element analysis, genetic algorithm

Date received: 14 January 2018; accepted: 27 July 2018

Handling Editor: Pietro Scandura

Introduction

The study of plate-like structures can serve as a prerequisite for the analysis of the dynamic performance of more complicated structures.[1,2] A variety of approaches have accordingly been developed for the optimization of the natural frequencies of plate structures.[3] These methods include modification of the dimension of the plate,[4–6] addition of masses to the plate,[7] modification of the topology of the structure,[8,9] and so forth. The optimization targets are usually maximizing the fundamental natural frequency,[4,10] maximizing the difference between two particular natural frequencies,[9] and modifying the natural frequencies to some particular desired values.[11,12]

Among these optimizations, the approach of changing the given natural frequencies to some particular target values is valuable and can have extensive applications in engineering.[12] For instance, it can be applied to improve the acoustic behavior of the panel

[1]School of Architecture, Huaqiao University, Xiamen, P.R. China
[2]Department of Building Services Engineering, The Hong Kong Polytechnic University, Kowloon, Hong Kong

Corresponding author:
Cheuk Ming Mak, Department of Building Services Engineering, The Hong Kong Polytechnic University, Kowloon, Hong Kong.
Email: becmmak@polyu.edu.hk

sound absorbers[13] or music instruments.[14] It can also be used to the optimal design of vibro-impacting structures intended for energy harvesting applications,[15,16] where a vibration-based energy harvester generates higher output powers when it is working at the resonant frequency coinciding with the ambient source frequency. Moreover, it can be useful in the design of smart structural systems, since the structural natural frequencies significantly affect the performance of the sensor or actuator that is embedded into or surface bonded with structures.[17]

The plate's boundary condition is one of the most significant factors that affect the natural frequencies of a plate structure. Over the past few years, the dynamic analysis of plate structures with various boundary conditions has received considerable attention.[18,19] Approximate solution techniques[20,21] have been developed for the analysis of the effects of general boundary conditions. Among these techniques, the finite element method (FEM) has been widely considered and proved to be especially suitable for the structures with complex boundary conditions.[22–24] Based on the FEM method and genetic algorithm (GA), an optimization method has recently been developed by the authors for optimizing the natural frequencies of plate structures.[12] The optimization results demonstrate that the plate's natural frequencies can be effectively optimized even only modifying the plate's boundary conditions.[12] This kind of optimization techniques only require the modification of boundary supports and therefore can be extremely valuable when the given constraints do not allow modifying the body and appearance of the structure (e.g. the mass, dimension, shape, and surface of the plate).[12] However, this method is developed by neglecting the effects of fluid loading and is only suitable for plates in vacuum.

It is well known that the natural frequencies of structures in contact with or immersed in a heavy fluid (like water) are quite different from those in vacuo. The natural frequency changes because of the presence of the fluid should be carefully calculated and considered in the design of structures that are in contact with or immersed in fluid.[25] Even in a light fluid medium (like air), the effect of fluid loading is proved to be a significant factor in near-resonant frequency regions.[22]

This work is an extension of the authors' earlier work[12] on the natural frequency optimization of plate structures by considering arbitrary boundary conditions as optimization variables. The developed optimization method in this article takes into account the effects of fluid loading and is suitable for structural optimization in arbitrary fluid domains. Generally, the FEM, boundary element method (BEM) and GA are combined in the proposed method. The layout of this article is as follows. The coupled FEM-BEM model for the fluid-loaded plate natural frequency analysis is introduced in section "Hydroelastic vibration analysis model," as well as the validation of this model. The GA approach is briefly introduced in section "Optimization methodology," where the procedure of the FEM-BEM-GA combined optimization method is also present. In section "Illustrative examples," the numerical studies are conducted to examine the performance of the proposed optimization method, and a brief discussion of these studies is given in section "Discussion." Finally, section "Conclusion" presents the conclusions.

Hydroelastic vibration analysis model

Coupled FEM-BEM model

Consider a rectangular thin plate mounting on an infinite rigid baffle (see Figure 1). Both sides of the plate are in contact with fluid (fluid medium V1 and fluid medium V2). The plate is with arbitrary elastic boundary supports along the edges and its length, width, and thickness are L_x, L_y, and h, respectively.

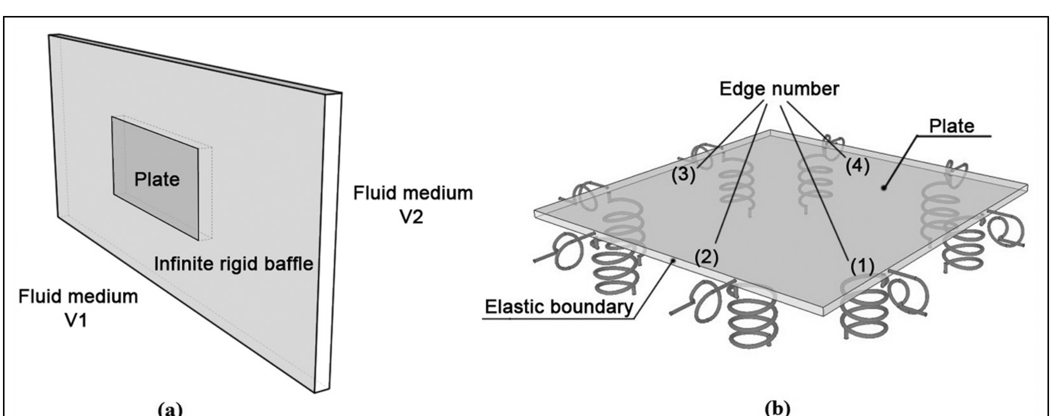

Figure 1. A fluid-loaded plate structure: (a) the front and back surfaces of the baffled plate are in contact with fluid media V1 and V2, respectively; (b) boundary condition of the plate.

The vibration response of the undamped plate system with fluid loading is determined by the coupled FEM-BEM method[18,26] as

$$\left(-\omega^2\{M\} + \{K\}\right)\{U\} = \{F\} + \{\mathscr{T}\}\left(\{P^+\} - \{P^-\}\right) \tag{1}$$

where ω is the natural angular frequency, $[M]$ is the plate's mass matrix, $[K]$ is the plate's stiffness matrix, $\{F\}$ is the external force applied on the plate, the vector $\{U\}$ represents the plate's nodal displacement, the vectors $\{P^+\}$ and $\{P^-\}$ are radiated sound pressures on the both sides of the plate surface (in medium V1 and in medium V2, respectively), and the transformation matrix $\{\mathscr{T}\}$ is used to convert the sound pressure to the nodal force acting on the plate.

The sound pressures on the both sides of the plate surface by the BEM model can be given as[18,22,27,28]

$$\{P^+\} = \{H^+\}\{w\} \tag{2}$$

$$\{P^-\} = -\{H^-\}\{w\} \tag{3}$$

where $\{H^+\}$ and $\{H^-\}$ are square matrices formed by the "collocation" procedure and are used to describe the fluid loading effects on the front (in medium V1) and back (in medium V2) plate surfaces, respectively. $\{w\} = \{\mathscr{R}\}\{U\}$ represents the transverse deflection vector, where the transformation matrix $\{\mathscr{R}\}$ is used to convert the nodal displacement vector to the transverse deflection vector.[18,22] Combining equations (1)–(3), the force–displacement relationship of the plate system can be given as

$$\left(-\omega^2\{M\} + \{K\} - \{\mathscr{T}\}\left(\{H^+\} + \{H^-\}\right)\{\mathscr{R}\}\right)\{U\} = \{F\} \tag{4}$$

The characteristic equation of the plate system can then be given as

$$\left(-\omega^2\{M\} + \{K\} - \{\mathscr{T}\}\left(\{H^+\} + \{H^-\}\right)\{\mathscr{R}\}\right)\{\varphi\} = \{0\} \tag{5}$$

The eigenvalue ω^2 and the eigenvector $\{\varphi\}$ can now be obtained from equation (5), which has taken into account the effect of fluid loading by the coupled FEM-BEM method.

In order to consider arbitrary boundary conditions, the stiffness matrix $\{K\}$ of the whole plate structure is decomposed into plate and boundary supports, and is given as[18]

$$\{K\} = \{K_p\} + \{K_b\} \tag{6}$$

where $\{K_p\}$ represents the stiffness matrix for the plate body and $\{K_b\}$ represents the stiffness matrix for the boundary supports. In general, the mass properties of the boundary supports can be neglected.[19,20,29] Therefore, the mass matrix $\{M\}$ of the whole plate structure only contains the mass matrix of the plate body, and can be expressed as

$$\{M\} = \{M_p\} \tag{7}$$

The elastic supports, as in references,[22–24] are modeled as a combination of translational and rotational springs, with k_{tb} and k_{rb} being the translation stiffness and rotational stiffness, respectively.

In the FEM model, the total strain energy Π_e of the whole plate element can be given by

$$\Pi_e = \Pi_{pe} + \Pi_{be} \tag{8}$$

where the stain energy of the plate body element Π_{pe} and the stain energy of the boundary support in the plate element $\Pi_{\rm be}$ can be expressed by

$$\Pi_{pe} = \frac{1}{2}\{U\}_e^T\{K_p\}_e\{U\}_e \tag{9}$$

and

$$\Pi_{be} = \frac{1}{2}\{U\}_e^T\{K_b\}_e\{U\}_e \tag{10}$$

$\{U\}_e$ is the nodal displacement vector of the element. $\{K_p\}_e$ and $\{K_b\}_e$ are the element stiffness matrices of $\{K_p\}$ and $\{K_b\}$, which can be expressed by[18,26]

$$\{K_p\}_e = \int \{B_p\}^T\{D_p\}\{B_p\}dxdy \tag{11}$$

and

$$\{K_b\}_e = \int\left(k_{tb}\{N_w\}^T\{N_w\} + k_{rb}\left\{\frac{\partial N_w}{\partial \vec{n}_b}\right\}^T\left\{\frac{\partial N_w}{\partial \vec{n}_b}\right\}\right)d\Gamma_b \tag{12}$$

where $\{B_p\}$ is the plate's strain matrix, $\{D_p\}$ is the plate's flexural rigidity matrix, $\{N_w\}$ is the shape function vector for the plate element, and $\vec{n}_b$ represents the normal unit vector of the element boundary contour Γ_b. The total kinetic energy T_e of the plate element is given by

$$T_e = \frac{1}{2}\{\dot{U}\}_e^T\{M_p\}_e\{\dot{U}\}_e \tag{13}$$

where $\{M_p\}_e$ is the element mass matrices of $\{M_p\}$, given by

$$\{M_p\}_e = \rho_p h\int\{N_w\}^T\{N_w\}dxdy \tag{14}$$

where ρ_p is the plate's density.

Table 1. NAVMI factors for clamped plates of different aspect ratios in contact with water.

Aspect ratios *Lx/Ly*	Method	NAVMI factor Γ_{mn}			
		$\Gamma_{1,1}$	$\Gamma_{1,2}$	$\Gamma_{2,1}$	$\Gamma_{2,2}$
1	Present study	0.349	0.157	0.157	0.114
	Kwak[30]	0.350	0.160	0.160	0.119
1.5	Present study	0.425	0.213	0.168	0.135
	Kwak[30]	0.423	0.215	0.173	0.139
2.0	Present study	0.485	0.259	0.174	00.149
	Kwak[30]	0.478	0.261	0.180	0.154
2.5	Present study	0.535	0.300	0.1782	0.158
	Kwak[30]	0.522	0.300	0.185	0.162
3.0	Present study	0.578	0.335	0.181	0.165
	Kwak[30]	0.559	0.333	0.187	0.171

NAVMI: non-dimensional added virtual mass increment.

The boundary parameters (k_{tb} and k_{rb}) in equation (12) can arbitrarily be varied from 0 to ∞ to simulate arbitrary elastic boundary conditions.

Model validation

The first four fundamental modes of a clamped rectangular plate (with different aspect ratios) in contact with water are predicted using the proposed coupled FEM-BEM model. In the calculations, the element number used is 32×32. The results are compared with the existing results given by Kwak,[30] which are given in Table 1. For convenient comparison, the natural frequency results are converted into NAVMI (non-dimensional added virtual mass incremental) factors, which are the same as those given by Kwak. The NAVMI factor, defined as $\Gamma = \left(\frac{f_v^2}{f_f^2} - 1\right)\frac{\rho_p h}{\rho_f L_x}$, is a non-dimensional parameter for characterizing the difference in the natural frequencies of the structure in vacuo and in contact with fluid, where f_v and f_f are the natural frequencies in vacuo and in fluid, respectively, ρ_f is the density of the fluid. Good agreement can be seen between the calculation results and those of the previous study.

Optimization methodology

There are at least two challenges in developing an optimization method that can be used to regulate the plate's multiple natural frequencies by optimizing the boundary conditions.[12] One is that multiple boundary parameters need to be optimized simultaneously and each of them can take on an infinite number of possible values. The other is that multiple natural frequencies are supposed to be optimized simultaneously; however, every slight change of the boundary conditions leads to a new value of each natural frequency. To deal with these difficulties, intelligent optimization techniques that can perform a parallel search in the possible solution spaces are required. In this work, a GA method is adopted and combined with the proposed FEM-BEM method for the development of optimization model.

GA

GA is a bionic algorithm inspired by natural evolution which is especially suitable for parallelizing the algorithm since the calculations of each generation are independent of one another.[12,31–33] As one type of metaheuristic algorithms, GA works by iteratively improving themselves with past data after each iteration rather than performing a stochastic or exhaustive search. Initialization, crossover, selection, and mutation are four basic bio-inspired operators used in the procedure of GA. The initialization process generates the initial population randomly. The population then evolves by the last three bio-inspired operators (i.e. crossover, selection, and mutation). Selection operator selects excellent individuals in the current generation for breeding the next generation individuals. To avoid local convergence, the mutation operator changes one or more gene value in a chromosome for individuals in the next generation. In the whole process, evaluation operator weights the fitness (quality) of individuals in each generation. The fitness function used in this work is given as

$$\text{Minimize } \Delta = \sum\left(W_n\left(\left|\frac{f_n - f_n^{target}}{f_n^{target}}\right|\right)\right) \tag{15}$$

where f_n and f_n^{target} are the nth order natural frequency and its target value, respectively. W_n is the weighting coefficient indicating the relative importance of the nth objective. This is the simplest objective function that aggregates the multiple natural frequency objectives into one weighted objective function.[12]

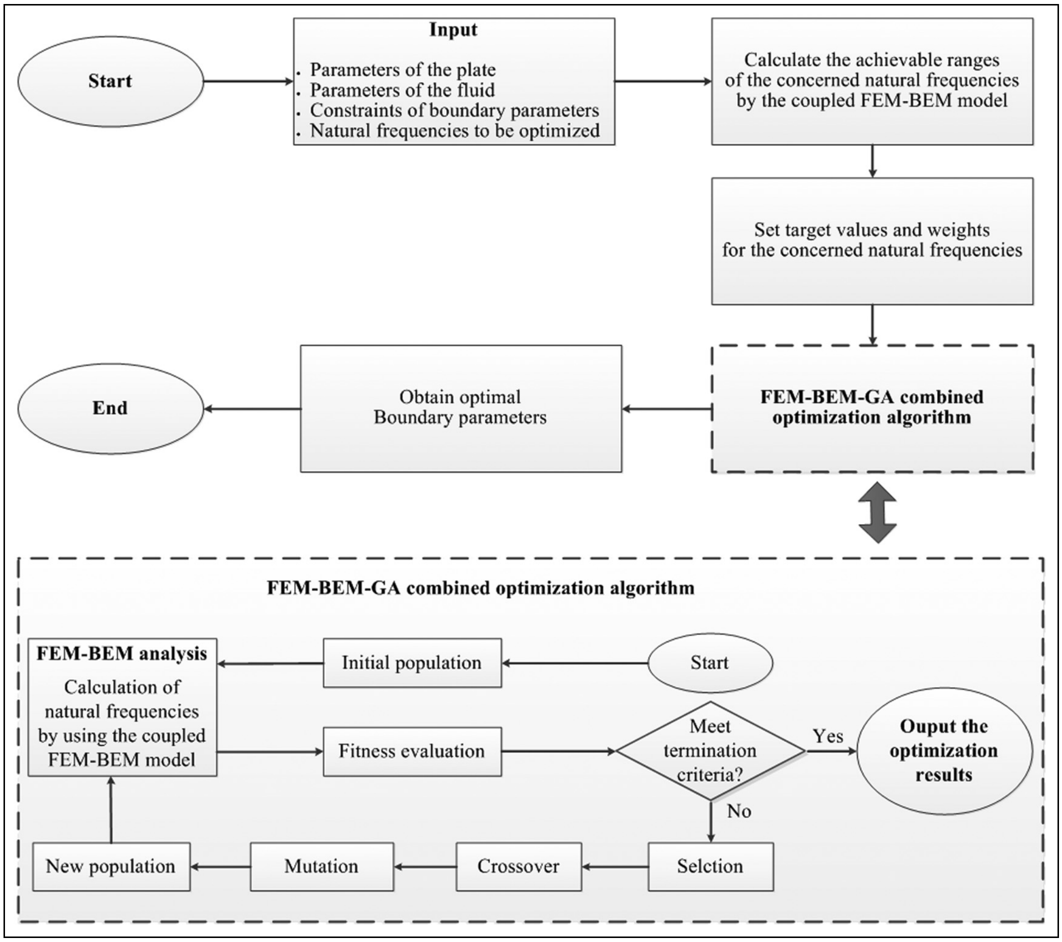

Figure 2. Flowchart of FEM-BEM-GA integrated optimization method.

FEM-BEM-GA integrated optimization approach

Figure 2 shows the flowchart of the optimization strategy, in which the GA and the coupled FEM-BEM method are combined. The procedure includes (a) inputting the plate's known parameters (such as size and density), the parameters of the fluid environment (such as the density and sound speed) on each side of the plate, and the constraints of the plate's boundary parameters; (b) identifying the natural frequencies to be optimized, and calculating their possible ranges under the given constraints of boundary parameters (using the coupled FEM-BEM method); (c) setting target values within their possible ranges for each natural frequency of interest, as well as their corresponding weighting coefficients; and (d) defining the termination criteria and running the FEM-BEM-GA combined method to get the optimal solutions.

Illustrative examples

Based on the proposed method, four optimization examples of fluid-loaded plate structures are presented in this section. The parameters used in these examples are as follows. (a) The element number used in the coupled FEM-BEM model is 32 × 32 (the same as in section "Hydroelastic vibration analysis model"). (b) The infinite large value of boundary parameter is represented by 1×10^{10}. (c) The initial population and maximum generation number defined in the GA are 100 and 1000, respectively. (d) The termination criterion is that the program terminates when $\left|\frac{f_n - f_n^{target}}{f_n^{target}}\right| \leq 1\%$ is reached for each natural frequencies of interest or when the predefined maximum number of iteration is reached.

Case 1

In this case, the plate in contact with water on one side is considered. The medium V1 is air and medium V2 is water (see Figure 1). The parameters of the plate and fluid media are given in Table 2. The constraints of boundary conditions of the plate are also given in the table, where $\bar{k}_{tb}$ and $\bar{k}_{rb}$ are the dimensionless forms of k_{tb} and k_{rb}, respectively.[19,34] The four edges of the plate are numbered and also shown in Figure 1.

Table 2. Known parameters of case 1.

Plate parameters							
Density (kg/m3)	Young's modulus (GPa)	Poisson's ratio	*Lx* (m)		*Ly* (m)		*h* (mm)
7800	216	0.28	1		0.75		5
Fluid parameters							
Fluid medium V1					Fluid medium V2		
Density (kg/m3) 1.21			Sound speed (m/s) 344		Density (kg/m3) 1000	Sound speed (m/s) 1483	
Boundary conditions							
Edge no.	1		2		3		4	
Boundary parameter	$\bar{k}_{tb1}$	$\bar{k}_{rb1}$	$\bar{k}_{tb2}$	$\bar{k}_{rb2}$	$\bar{k}_{tb3}$	$\bar{k}_{rb3}$	$\bar{k}_{tb4}$	$\bar{k}_{rb4}$
Variable range	∞	0–1000	∞	0–1000	∞	0–1000	∞	0–1000

Table 3. Optimization target and optimal results of case 1

Optimization target	Natural frequencies to be optimized	f_1 and f_2
	Achievable range (Hz)	$f_1 \in [10.96, 21.61]$, $f_2 \in [31.44, 49.12]$
	Target values (Hz)	$f_1^{target} = 15$, $f_2^{target} = 40$
	Weights	$W_1 = 1, W_2 = 1$
Optimization result	Boundary condition	$\bar{k}_{tb1} = \infty, \bar{k}_{rb1} = 0, \bar{k}_{tb2} = \infty, \bar{k}_{rb2} = 213.95,$ $\bar{k}_{tb3} = \infty, \bar{k}_{rb3} = 4.29, \bar{k}_{tb4} = \infty, \bar{k}_{rb4} = 21.69$
	Natural frequencies (Hz)	$f_1 = 15.14, f_2 = 39.70$
Percentage deviation	$\left\lvert\frac{f_n - f_n^{target}}{f_n^{target}}\right\rvert \leqslant 1\%$ ($n = 1, 2$)	

Table 4. Optimization targets and results of case 2.

Optimization target	Natural frequencies to be optimized	f_1 and f_4
	Achievable range (Hz)	$f_1 \in [10.96, 21.61]$, $f_4 \in [67.84, 92.48]$
	Target values (Hz)	$f_1^{target} = 18$, $f_4^{target} = 85$
	Weights	$W_1 = 1$, $W_4 = 1$
Optimization result	Boundary condition	$\bar{k}_{tb1} = \infty, \bar{k}_{rb1} = 76.92, \bar{k}_{tb2} = \infty, \bar{k}_{rb2} = 80.04,$ $\bar{k}_{tb3} = \infty, \bar{k}_{rb3} = 37.74, \bar{k}_{tb4} = \infty, \bar{k}_{rb4} = 5.03$
	Natural frequencies (Hz)	$f_1^{target} = 17.83$, $f_4^{target} = 85.04$
Percentage deviation	$\left\lvert\frac{f_n - f_n^{target}}{f_n^{target}}\right\rvert \leqslant 1\%$ ($n = 1, 4$)	

The optimization target is given in Table 3. The concerned natural frequencies are f_1 and f_2. Based on the known parameters given in Table 2, the achievable ranges for f_1 and f_2 can be easily determined by the proposed coupled FEM-BEM method, which are 10.96–21.61 and 31.44–49.12 Hz, respectively. The target values for these two frequencies are set to 15 and 40 Hz, respectively, and their associated weighting coefficients are both set to 1.

For this case, as also shown in Table 3, the optimal boundary parameters are found to be $\bar{k}_{tb1} = \infty$, $\bar{k}_{rb1} = 0$, $\bar{k}_{tb2} = \infty$, $\bar{k}_{rb2} = 213.95$, $\bar{k}_{tb3} = \infty$, $\bar{k}_{rb3} = 4.29$, $\bar{k}_{tb4} = \infty$, and $\bar{k}_{rb4} = 21.69$, which can adjust f_1 and f_2 to 15.14 and 39.70 Hz, respectively. Their percentage deviations from the target values are both smaller than 1%.

Case 2

The parameters of the plate, fluid media, and constraints of boundary conditions in this case are the same as those in case 1 (also see Table 2), but the concerned natural frequencies are changed to be f_1 and f_4.

The optimization target is given in Table 4. The concerned natural frequencies are f_1 and f_4. Based on the known parameters given in Table 2, the achievable

Table 5. Known parameters of case 3.

Plate parameters									
Density (kg/m3)	Young's modulus (GPa)		Poisson's ratio	Lx (m)		Ly (m)		h (mm)	
2700	68.5		0.34	0.8		0. 5		4	
Fluid parameters									
Fluid medium V1						Fluid medium V2			
Density (kg/m3) 1000				Sound speed (m/s) 1483		Density (kg/m3) 1000		Sound speed (m/s) 1483	
Boundary conditions									
Edge no.	1			2		3		4	
Boundary parameter	$\bar{k}_{tb1}$	$\bar{k}_{rb1}$		$\bar{k}_{tb2}$	$\bar{k}_{rb2}$	$\bar{k}_{tb3}$	$\bar{k}_{rb3}$	$\bar{k}_{tb4}$	$\bar{k}_{rb4}$
Variable range	100–1000	0–1000		100–1000	0–1000	100–1000	0–1000	100–1000	0–1000

Table 6. Optimization targets and results of case 3.

Optimization target	Natural frequencies to be optimized	f_1, f_2, and f_3
	Achievable range (Hz)	$f_1 \in [3.73, 10.21]$, $f_2 \in [8.22, 19.60]$, $f_3 \in [11.27, 28.28]$
	Target values (Hz)	$f_1^{target} = 6$, $f_2^{target} = 12$, $f_3^{target} = 18$
	Weights	$W_1 = 1$, $W_2 = 0.8$, $W_3 = 0.6$
Optimization result	Boundary condition	$\bar{k}_{tb1} = 128.38, \bar{k}_{rb1} = 12.49, \bar{k}_{tb2} = 549.58, \bar{k}_{rb2} = 447.70,$ $\bar{k}_{tb3} = 100.00, \bar{k}_{rb3} = 0, \bar{k}_{tb4} = 526.56, \bar{k}_{rb4} = 766.08$
	Natural frequencies (Hz)	$f_1 = 5.97$, $f_2 = 11.92$, $f_3 = 17.97$
Percentage deviation	$\left\lvert\frac{f_n - f_n^{target}}{f_n^{target}}\right\rvert \leqslant 1\%$ ($n = 1, 2, 3$)	

ranges for f_1 and f_4 can be determined as 10.96–21.61 and 67.84–92.48 Hz, respectively. The target values for these two frequencies are 18 and 85 Hz, respectively, and their associated weighting coefficients are both set to 1.

For this case, as also shown in Table 4, the optimal boundary parameters are found to be $\bar{k}_{tb1} = \infty$, $\bar{k}_{rb1} = 76.92$, $\bar{k}_{tb2} = \infty$, $\bar{k}_{rb2} = 80.04$, $\bar{k}_{tb3} = \infty$, $\bar{k}_{rb3} = 37.74$, $\bar{k}_{tb4} = \infty$, and $\bar{k}_{rb4} = 5.03$, which can adjust f_1 and f_4 to 17.83 and 85.04 Hz, respectively. Their percentage deviations from the target values are both smaller than 1%.

Case 3

In this case, the plate fully immersed in the water (i.e. both sides of the plate are in contact with water) is considered. The parameters of the plate and fluid media are given in Table 5, as well as the constraints of boundary conditions.

The optimization target is given in Table 6. The concerned natural frequencies are f_1, f_2, and f_3. Based on the known parameters given in Table 5, the achievable ranges for f_1, f_2, and f_3 can be determined as 3.73–10.21, 8.22–19.60, and 11.27–28.28 Hz, respectively. The target values for these three frequencies are 6, 12, and 18 Hz, respectively, and their associated weighting coefficients are set to 1, 0.8, and 0.6, respectively.

For this case, as also shown in Table 6, the optimal boundary parameters are found to be $\bar{k}_{tb1} = 128.38$, $\bar{k}_{rb1} = 12.49$, $\bar{k}_{tb2} = 549.58$, $\bar{k}_{rb2} = 447.70$, $\bar{k}_{tb3} = 100.00$, $\bar{k}_{rb3} = 0$, $\bar{k}_{tb4} = 526.56$, and $\bar{k}_{rb4} = 766.08$, which can adjust f_1, f_2, and f_3 to 5.97, 11.92, and 17.97 Hz, respectively. Their percentage deviations from the target values are all smaller than 1%.

Case 4

The parameters of the plate in this case are shown in Table 7. The plate is fully immersed in the water, that is, both sides of the plate are in contact with water. The optimization targets are shown in Table 8. The concerned natural frequencies are f_1, f_2, f_3, and f_4. Based on the given parameters in Table 7, the achievable ranges for f_1, f_2, f_3, and f_4 can be determined as 2.25–15.82, 4.93–28.93, 11.43–48.63, and 21.33–66.13 Hz, respectively. The target values for these frequencies are 5, 10, 15, and 25 Hz, respectively. Two sets of weighting coefficients ($W_1 = 1, W_2 = 1, W_3 = 0.5, W_4 = 0.5$ and $W_1 = 0.5, W_2 = 0.5, W_3 = 1, W_4 = 1$) are considered in this case.

Table 7. Known parameters of case 4.

Plate parameters							
Density (kg/m3)	Young's modulus (GPa)	Poisson's ratio		Lx (m)		Ly (m)	h (mm)
2500	65	0.25		0.75		0.4	3
Fluid parameters							
Fluid medium V1						Fluid medium V2	
Density (kg/m3) 1000			Sound speed (m/s) 1483			Density (kg/m3) 1000	Sound speed (m/s) 1483
Boundary conditions							
Edge no.	1		2		3		4	
Boundary parameter	$\bar{k}_{tb1}$	$\bar{k}_{rb1}$	$\bar{k}_{tb2}$	$\bar{k}_{rb2}$	$\bar{k}_{tb3}$	$\bar{k}_{rb3}$	$\bar{k}_{tb4}$	$\bar{k}_{rb4}$
Variable range	∞	∞	0–∞	0–∞	0–∞	0–∞	0–∞	0–∞

Table 8. Optimization targets and results of case 4.

Optimization target	Natural frequencies to be optimized	f_1, f_2, f_3, and f_4	
	Achievable range (Hz)	$f_1 \in [2.25, 15.82], f_2 \in [4.93, 28.93]$, $f_3 \in [11.43, 48.63], f_4 \in [21.33, 66.13]$	
	Target values (Hz)	$f_1^{target} = 5, f_2^{target} = 10, f_3^{target} = 15, f_4^{target} = 25$	
	Weights	$W_1 = 1, W_2 = 1, W_3 = 0.5, W_4 = 0.5$	$W_1 = 0.5, W_2 = 0.5, W_3 = 1, W_4 = 1$
Optimization result	Boundary condition	$\bar{k}_{tb1} = \infty, \bar{k}_{rb1} = \infty$ $\bar{k}_{tb2} = 469.19, \bar{k}_{rb2} = 4210.51$ $\bar{k}_{tb3} = 136.28, \bar{k}_{rb3} = 0$ $\bar{k}_{tb4} = 49.56, \bar{k}_{rb4} = 2.33$	$\bar{k}_{tb1} = \infty, \bar{k}_{rb1} = \infty$ $\bar{k}_{tb2} = 145.37, \bar{k}_{rb2} = 0$ $\bar{k}_{tb3} = 45.34, \bar{k}_{rb3} = 0$ $\bar{k}_{tb4} = 80.49, \bar{k}_{rb4} = 2.19$
	Natural frequencies (Hz)	$f_1 = 5.00, f_2 = 10.00$ $f_3 = 17.45, f_4 = 25.00$	$f_1 = 5.00, f_2 = 8.70$ $f_3 = 15.00, f_4 = 25.01$
Percentage deviation $\left\lvert \frac{f_n - f_n^{\text{target}}}{f_n^{\text{target}}} \right\rvert$		0.00%, 0.00%, 16.37%, and 0.00% for n = 1, 2, 3, and 4, respectively.	0.00%, 13.00%, 0.00%, and 0.03% for n = 1, 2, 3, and 4, respectively.

For this case, as also shown in Table 8, for the first set of weighting coefficients, the optimal boundary parameters are found to be $\bar{k}_{tb1} = \infty$, $\bar{k}_{rb1} = \infty$, $\bar{k}_{tb2} = 469.19$, $\bar{k}_{rb2} = 4210.51$, $\bar{k}_{tb3} = 136.28$, $\bar{k}_{rb3} = 0$, $\bar{k}_{tb4} = 49.56$, and $\bar{k}_{rb4} = 2.33$, which can adjust f_1, f_2, f_3, and f_4 to 5.00, 10.00, 17.45, and 25.00 Hz, respectively. Their percentage deviations from the target values are 0.00%, 0.00%, 16.37%, and 0.00%, respectively. For the second set of weighting coefficients, the optimal boundary parameters are found to be $\bar{k}_{tb1} = \infty$, $\bar{k}_{rb1} = \infty$, $\bar{k}_{tb2} = 145.37$, $\bar{k}_{rb2} = 0$, $\bar{k}_{tb3} = 45.34$, $\bar{k}_{rb3} = 0$, $\bar{k}_{tb4} = 80.49$, and $\bar{k}_{rb4} = 2.19$, which can adjust f_1, f_2, f_3, and f_4 to 5.00, 8.70, 15.00, and 25.01 Hz, respectively. Their percentage deviations from the target values are 0.00%, 13.00%, 0.00%, and 0.03%, respectively.

Discussion

The plate's actual natural frequencies are highly related to its boundary conditions. For instance, in each of the above calculation cases, the values of the plate's target natural frequencies can be adjusted within a relatively wide range, even only considering its boundary parameters as design variables. In addition, with different target natural frequencies, although the given plate and fluid parameters are totally the same, the values of optimal boundary parameters of case 1 and case 2 are found to be quite different.

The fluid loading effect is another important factor that significantly influences the plate's natural frequencies. Taking case 3 as an example, with all the known parameters remaining the same but considering the plate immersed in the air, the achievable ranges of f_1,f_2, and f_3 are [26.83, 71.23], [41.51, 99.10], and [49.54, 126.43], respectively, which are quite different from those of the same plate immersed in the water ([3.73, 10.21],[8.22, 19.60], and [11.27, 28.28], respectively) (see Table 6).

The GA is suitable for the optimization problem considered in this study. Taking case 4 as an example, six boundary parameters are set as the optimization variables and each of them has an infinite number of possible values. Moreover, natural frequencies of four different orders need to be optimized to their responding target values at the same time. It is impossible or extremely difficult to conduct a traditional search for these tasks. The adoption of the intelligent search algorithm (GA) in the proposed method is necessary and useful.

It is also worth mentioning that in some specific cases (e.g. case 4), it cannot guarantee to optimize all the concerned natural frequencies to be exactly the target values by changing the boundary conditions within the predefined search space. However, even in this situation, the optimization approach can help establish the optimal boundary conditions which can minimize the value of the weighted objective function (i.e. ensure the multiple natural frequencies of interest to be as close to their corresponding targets as possible). In this situation, the selected weighting coefficients will influence the final results of the optimization.

In a word, the results of the numerical studies above demonstrate that (a) every natural frequency of a given fluid-loaded plate is sensitive to its actual boundary conditions; (b) the plate's multiple natural frequencies can be effectively optimized even only taking its boundary conditions as design variables; (c) users can consider arbitrary fluid loading using the proposed method; and (d) users can freely set the constraints of the plate's boundary conditions according to practical needs, and identify the optimal boundary conditions within these constraints according to their natural frequency targets.

Conclusion

An optimization approach is developed for the optimization of natural frequencies of fluid-loaded plates using the FEM, BEM, and GA combined method. In this approach, the coupled FEM-BEM method is employed for the free flexural vibration analysis of plates and is demonstrated to be suitable for studying the effects of arbitrary elastic boundary conditions and arbitrary fluid loading. Moreover, the GA is combined with the coupled FEM-BEM method for determining the optimal values of plate's boundary parameters.

Parametric studies are carried out. The results demonstrate the proposed optimization approach can effectively identify the optimal boundary parameters so that multiple natural frequencies of a given fluid-loaded plate can be adapted at the same time to their corresponding targets. To our knowledge, the proposed method is the first algorithm that can optimize fluid-loaded plate natural frequencies by considering arbitrary boundary conditions as optimization variables; hence, the idea and the method proposed in this work can be useful for both academic and practical applications.

Declaration of conflicting interests

The author(s) declared no potential conflicts of interest with respect to the research, authorship, and/or publication of this article.

Funding

The author(s) disclosed receipt of the following financial support for the research, authorship, and/or publication of this article: The work was supported by the National Natural Science Foundation of China (51578252), Program for New Century Excellent Talents in Fujian Province University (2017), a grant from the Hong Kong Polytechnic University (PolyU Project account: G-YBFP), and High Level Talent Innovation and Entrepreneurship Program of Quanzhou City, China (2017G039).

ORCID iD

Dayi Ou https://orcid.org/0000-0003-2110-9382

References

1. Zaidi AMA, Koslan MFS, Othman MZ, et al. Appropriate coupling solvers for the numerical simulation of rolled homogeneous armor plate response subjected to blast loading. *Adv Mech Eng* 2013; 2013: 637564.
2. Kang SW and Atluri SN. Improved non-dimensional dynamic influence function method for vibration analysis of arbitrarily shaped plates with clamped edges. *Adv Mech Eng* 2016; 8: 247–253.
3. Zargham S, Ward TA, Ramli R, et al. Topology optimization: a review for structural designs under vibration problems. *Struct Multidiscip O* 2016; 53: 1157–1177.
4. Moradi R, Vaseghi O and Mirdamadi HR. Constrained thickness optimization of rectangular orthotropic fiber-reinforced plate for fundamental frequency maximization. *Optim Eng* 2014; 15: 293–310.
5. Mirzaeifar R, Shahab S and Bahai H. An approximate method for simultaneous modification of natural frequencies and buckling loads of thin rectangular isotropic plates. *Eng Struct* 2009; 31: 208–215.
6. Park M, Park Y and Park Y. Raising natural frequencies of a structure via surface-grooving technique. *Struct Multidiscip O* 2007; 34: 491–505.
7. Rubio L, Fernandez-Saez J and Morassi A. Point mass identification in rectangular plates from minimal natural frequency data. *Mech Syst Signal Pr* 2016; 80: 245–261.

8. El-Sabbagh A, Akl W and Baz A. Topology optimization of periodic Mindlin plates. *Finite Elem Anal Des* 2008; 44: 439–449.
9. Zhao CB, Steven GP and Xie YM. Evolutionary optimization of maximizing the difference between two natural frequencies of a vibrating structure. *Struct Optimization* 1997; 13: 148–154.
10. Tsai TD and Cheng CC. Structural design for desired eigenfrequencies and mode shapes using topology optimization. *Struct Multidiscip O* 2013; 47: 673–686.
11. Zhao CB, Steven GP and Xie YM. Simultaneously evolutionary optimization of several natural frequencies of a two dimensional structure. *Struct Eng Mech* 1999; 7: 447–456.
12. Ou D and Mak CM. Optimization of natural frequencies of a plate structure by modifying boundary conditions. *J Acoust Soc Am* 2017; 142: EL56.
13. Zhao X and Fan X. Enhancing low frequency sound absorption of micro-perforated panel absorbers by using mechanical impedance plates. *Appl Acoust* 2015; 88: 123–128.
14. Miao Y, Liu Z, Liu Y, et al. Effect of vibration properties of a resonance board on piano timbre. *Forest Prod J* 2016; 66: 126–133.
15. Ostasevicius V, Janusas G, Milasauskaite I, et al. Peculiarities of the third natural frequency vibrations of a cantilever for the improvement of energy harvesting. *Sensors* 2015; 15: 12594–12612.
16. Zizys D, Gaidys R, Dauksevicius R, et al. Segmentation of a vibro-shock cantilever-type piezoelectric energy harvester operating in higher transverse vibration modes. *Sensors* 2016; 16: 11.
17. Her S and Lin C. Vibration analysis of composite laminate plate excited by piezoelectric actuators. *Sensors* 2013; 13: 2997–3013.
18. Ou DY. Low frequency sound insulation analysis and evaluation of stiffened building structures. *Build Environ* 2015; 94: 802–809.
19. Li WL. Vibration analysis of rectangular plates with general elastic boundary supports. *J Sound Vib* 2004; 273: 619–635.
20. Chiello O, Sgard FC and Atalla N. On the use of a component mode synthesis technique to investigate the effects of elastic boundary conditions on the transmission loss of baffled plates. *Comput Struct* 2003; 81: 2645–2658.
21. Ou DY and Mak CM. A review of prediction methods for the transient vibration and sound radiation of plates. *J Low Freq Noise V A* 2013; 32: 309–322.
22. Ou DY and Mak CM. Experimental validation of the sound transmission of rectangular baffled plates with general elastic boundary conditions. *J Acoust Soc Am* 2011; 129: EL274–EL279.
23. Ou DY and Mak CM. The effects of elastic supports on the transient vibroacoustic response of a window caused by sonic booms. *J Acoust Soc Am* 2011; 130: 783–790.
24. Ou DY and Mak CM. Minimizing the transient vibroacoustic response of a window to sonic booms by using stiffeners (L). *J Acoust Soc Am* 2014; 135: 1672–1675.
25. Kerboua Y, Lakis AA, Thomas M, et al. Vibration analysis of rectangular plates coupled with fluid. *Appl Math Model* 2008; 32: 2570–2586.
26. Ou DY, Mak CM and Deng SM. Prediction of the sound transmission loss of a stiffened window. *Build Serv Eng Res T* 2013; 34: 359–368.
27. Wu TW. *Boundary element acoustics: fundamentals and computer codes*. Boston, MA: WIT Press, 2000.
28. Herrin DW, Martinus F, Wu TW, et al. An assessment of the high frequency boundary element and Rayleigh integral approximations. *Appl Acoust* 2006; 67: 819–833.
29. Park J, Mongeau L and Siegmund T. Influence of support properties on the sound radiated from the vibrations of rectangular plates. *J Sound Vib* 2003; 264: 775–794.
30. Kwak MK. Hydroelastic vibration of rectangular plates. *J Appl Mech: T ASME* 1996; 63: 110–115.
31. Haupt RL and Haupt SE. *Practical genetic algorithms*. 2nd ed. Hoboken, NJ: John Wiley & Sons, 2004.
32. Li D, Zigoneanu L, Popa B, et al. Design of an acoustic metamaterial lens using genetic algorithms. *J Acoust Soc Am* 2012; 132: 2823–2833.
33. Karakaya S and Soykasap O. Natural frequency and buckling optimization of laminated hybrid composite plates using genetic algorithm and simulated annealing. *Struct Multidiscip O* 2011; 43: 61–72.
34. Li WL, Zhang X, Du J, et al. An exact series solution for the transverse vibration of rectangular plates with general elastic boundary supports. *J Sound Vib* 2009; 321: 254–269.

Appendix 1

Notation

L_x	plate length
L_y	plate width
h	plate thickness
$\{B_p\}$	strain matrix of plate
$\{D_p\}$	flexural rigidity of plate
$\{N_w\}$	shape function vector
$\vec{n}_b$	normal unit vector
ω	frequency in radian
$[M]$	mass matrix of whole plate structure
$\{M_p\}$	mass matrix of plate body
$\{M_p\}_e$	element mass matrix of plate body
$[K]$	stiffness matrix of whole plate structure
$\{K_p\}$	stiffness matrix of plate body
$\{K_p\}_e$	element stiffness matrix of plate body
$\{K_b\}$	stiffness matrix of plate boundary supports
$\{K_b\}_e$	element stiffness matrix of plate boundary supports
k_{tb}	translational stiffness of plate boundary
k_{rb}	rotational stiffness of plate boundary
$\{F\}$	external force
$\{P^+\}$, $\{P^-\}$	radiated sound pressure on plate surface

$\{H^+\}$, $\{H^-\}$	fluid loading effect matrix on plate surface	T_e	total kinetic energy of plate element
$\{w\}$	transverse deflection vector of plate	f_v	plate natural frequency in vacuo
$\{U\}$	nodal displacement of plate	f_f	plate natural frequency in fluid
$\{U\}_e$	element nodal displacement of plate	ρ_f	fluid density
$\{\mathscr{T}\}$, $\{\mathscr{R}\}$	transformation matrix	ρ_p	plate density
$\{\varphi\}$	eigenvector	Γ	NAVMI factor
Π_e	total strain energy of plate element	W_n	weighting coefficient
Π_{pe}	element strain energy of plate body	f_n	nth order natural frequency of plate structure
Π_{be}	element strain energy of boundary support	f_n^{target}	nth order target natural frequency of plate structure